

## EUROPEAN LABORATORY FOR PARTICLE PHYSICS

CERN-EP / 98-161

October 19, 1998

## Charmonia production in 450 GeV/c proton induced reactions

M.C. Abreu<sup>1,a)</sup>, C. Baglin<sup>2)</sup>, A. Baldit<sup>3)</sup>, M. Bedjidian<sup>4)</sup>, P. Bordalo<sup>1,b)</sup>,  
A. Bussière<sup>2)</sup>, P. Busson<sup>5)</sup>, J. Castor<sup>3)</sup>, T. Chambon<sup>3)</sup>, C. Charlot<sup>5)</sup>, B. Chaurand<sup>5)</sup>,  
D. Contardo<sup>4)</sup>, E. Descroix<sup>4,c)</sup>, A. Devaux<sup>3)</sup>, O. Drapier<sup>4)</sup>, B. Espagnon<sup>3)</sup>,  
J. Fargeix<sup>3)</sup>, R. Ferreira<sup>1)</sup>, F. Fleuret<sup>5)</sup>, P. Force<sup>3)</sup>, L. Fredj<sup>3)</sup>, J. Gago<sup>1,b)</sup>,  
C. Gerschel<sup>6)</sup>, P. Gorodetzky<sup>7,d)</sup>, J.Y. Grossiord<sup>4)</sup>, A. Guichard<sup>4)</sup>, J.P. Guillaud<sup>2)</sup>,  
R. Haroutunian<sup>4)</sup>, D. Jouan<sup>6)</sup>, L. Kluberg<sup>5)</sup>, R. Kossakowski<sup>2)</sup>, G. Landaud<sup>3)</sup>,  
C. Lourenço<sup>1,8)</sup>, R. Mandry<sup>4)</sup>, F. Ohlsson-Malek<sup>4,e)</sup>, J.R. Pizzi<sup>4)</sup>, C. Racca<sup>7)</sup>,  
S. Ramos<sup>1,b)</sup>, A. Romana<sup>5)</sup>, P. Saturnini<sup>3)</sup>, S. Silva<sup>1)</sup>, P. Sonderegger<sup>8,b)</sup>,  
X. Tarrago<sup>6)</sup>, J. Varela<sup>1,b,f)</sup>

*NA38 Collaboration*

### Abstract

Absolute  $J/\psi$  and  $\psi'$  production cross sections have been measured at the CERN SPS, with 450 GeV/c protons incident on a set of C, Al, Cu and W targets. Complementing these values with the results obtained by experiment NA51, which used the same beam and detector with H and D targets, we establish a coherent picture of charmonia production in proton-induced reactions at SPS energies. In particular, we show that the scaling of the  $J/\psi$  cross section with the mass number of the target,  $A$ , is well described as  $A^\alpha$ , with  $\alpha^\psi = 0.919 \pm 0.015$ . The ratio between the  $J/\psi$  and  $\psi'$  yields, in our kinematical window, is found to be independent of  $A$ , with  $\alpha^{\psi'} - \alpha^\psi = 0.014 \pm 0.011$ .

*Accepted by Physics Letters B*

- 
- 1) LIP, Av. Elias Garcia 14, P-1000 Lisbon, Portugal
  - 2) LAPP, IN2P3-CNRS, F-74941 Annecy-le-Vieux Cedex, France
  - 3) LPC Clermont-Ferrand, IN2P3-CNRS and Université Blaise Pascal, F-63177 Aubière Cedex, France
  - 4) IPN Lyon, IN2P3-CNRS and Université Claude Bernard, F-69622 Villeurbanne Cedex, France
  - 5) LPNHE, Ecole Polytechnique, IN2P3-CNRS, F-91128 Palaiseau Cedex, France
  - 6) IPN, IN2P3-CNRS and Université de Paris-Sud, F-91406 Orsay Cedex, France
  - 7) IRes, IN2P3-CNRS and Université Louis Pasteur, F-67037 Strasbourg Cedex, France
  - 8) CERN, CH-1211 Geneva 23, Switzerland
  - a) Also at FCUL, Universidade de Lisboa, Lisbon, Portugal
  - b) Also at IST, Universidade Técnica de Lisboa, Lisbon, Portugal
  - c) Now at Université Jean Monnet, Saint-Etienne, France
  - d) Now at PCC Collège de France, Paris, France
  - e) Now at ISN, Grenoble, France
  - f) Now at CERN, Geneva, Switzerland

# 1 Introduction

Since the  $J/\psi$  discovery, hadro-production of charmonium states has been extensively studied, in particular with proton beams incident on different nuclear targets and at several energies [1].

The NA38 experiment has been designed to study dimuon production in high energy nucleus-nucleus reactions. In particular, the study of  $J/\psi$  production is generally considered as one of the most promising methods to probe the formation of deconfined QCD matter in heavy ion collisions [2]. The measurements presented in this paper are aimed at establishing a reference baseline (the “normal” charmonium behaviour) relative to which the heavy ion specific features can be identified.

Ideally, the reference data should be collected with a proton beam of the same energy as that of the ion beams,  $\sim 200$  GeV. However, the primary SPS proton beam has 450 GeV/ $c$  momentum, and lower energies require secondary beams. The tagging of the pions contaminating a 200 GeV proton beam ( $\sim 30\%$ ) implies the use of threshold Cherenkov counters, too slow to be compatible with the high beam intensities required by the small cross section processes we want to study.

The data have been collected in 1988 and a first analysis can be found in [3], where extensive experimental details are discussed. This paper presents the results of a new data analysis, that follows the procedures recently used to analyze the S-U data [4], also collected by NA38, and the Pb-Pb data, collected by the NA50 experiment [5].

## 2 Apparatus and data reduction

The dimuon mass distributions, where the muon pairs from  $J/\psi$  and  $\psi'$  decays appear as prominent resonances, were collected with the muon spectrometer described in detail in Ref. [6]. The operation of the detector was optimised to collect a significant sample of charmonia events in a very limited amount of beam time.

The toroidal magnet of the spectrometer was operated with a current of 10 000 A. The magnetic field (average  $\int B dl = 3$  Tm) deflects the low momentum tracks from the roads that fulfill the trigger logic requirements. This strong reduction of the low mass dimuon yield allows to run with high beam intensities while keeping a trigger rate compatible with a low dead time of the data acquisition system. The analysing power of the spectrometer with this strong magnetic field allows to easily separate the  $J/\psi$  and  $\psi'$  peaks.

The hadrons produced in the target were prevented from reaching the muon chambers and trigger hodoscopes by 520 cm of carbon, equivalent to  $11 \lambda_{\text{int}}$ . Under these conditions, the dimuon mass resolution is  $\sim 85$  MeV at the  $J/\psi$  mass, mainly due to the effects of multiple scattering of the muons in the hadron absorber and to the vertex uncertainty within the (relatively long) targets.

The characteristics of the 6 cylindrical targets used in this study can be found in Table 1. Their transverse section was in all cases big enough to intercept 100 % of

the beam profile. Two sets of Cu and W data were collected, with targets of different lengths, to control the systematical effects related to the target thickness.

Table 1: Thickness, interaction length, density and mass number of the targets used. The value 173.43 takes into account the impurities of this W target.

	$L$ (cm)	$\lambda_{\text{int}}$ (cm)	$\rho$ (g/cm <sup>3</sup> )	A (g)
C	30.0	43.09	1.88	12.011
Al	20.0	37.88	2.70	26.982
Cu	2.0	14.61	8.96	63.546
Cu	10.1	14.61	8.96	63.546
W	1.5	9.819	17.80	173.43
W	5.6	9.306	19.1	183.85

The intensity of the incident beam,  $\sim 10^8$  protons per 2.4 s spill, was measured with a ionization chamber filled with argon, previously calibrated at low intensity. The linearity of its response was checked with Carbon foils activation measurements up to the highest beam intensities used. The targetting efficiency was continuously monitored with a set of three scintillator telescopes, pointing to the target, placed in the plane perpendicular to the beam axis.

The event selection criteria is described in detail in Ref. [3]. Events with any of the two reconstructed tracks traversing the iron poles of the magnet are rejected, since their additional multiple scattering would deteriorate the dimuon mass resolution. The standard geometrical and fiducial quality cuts were applied.

The number of background opposite-sign muon pairs,  $N_{\text{bg}}$ , originating from pion and kaon decays is computed from the sample of like-sign pairs according to the relation

$$N_{\text{bg}} = 2 \times R_{\text{bg}} \times \sqrt{N^{++} \times N^{--}} \quad ,$$

where  $N^{++}$  and  $N^{--}$  are the numbers of positive and negative like-sign muon pairs, respectively. The signal is extracted as  $N_{\text{signal}} = N^{+-} - N_{\text{bg}}$ , where  $N^{+-}$  is the number of measured opposite-sign events.

The  $R_{\text{bg}}$  factor is unity in the absence of any charge correlation effect in the yields of accepted opposite- and like-sign muon pairs. In the present analysis we have rejected those events where any of the muons would not had been accepted if it had the opposite charge. This ensures the absence of any trigger or acceptance bias in the probability to accept muon pairs with any charge combination. However, the charge correlation at the pion and kaon production level leads to a higher fraction of muon pairs with opposite charges, which translates into a  $R_{\text{bg}}$  factor bigger than unity. In this study we adopted  $R_{\text{bg}} = 1.25$  for all the data sets, with no distinction between light and heavy targets. It should be noted that the yield of background events amounts to less than 0.2% of the signal, in the  $J/\psi$  mass region and above.

The phase space window is defined by the following kinematical cuts: center of mass rapidity,  $y^*$ , between  $-0.4$  and  $0.6$ ;  $|\cos(\theta_{\text{cs}})| < 0.5$ , where  $\theta_{\text{cs}}$  is the muon polar

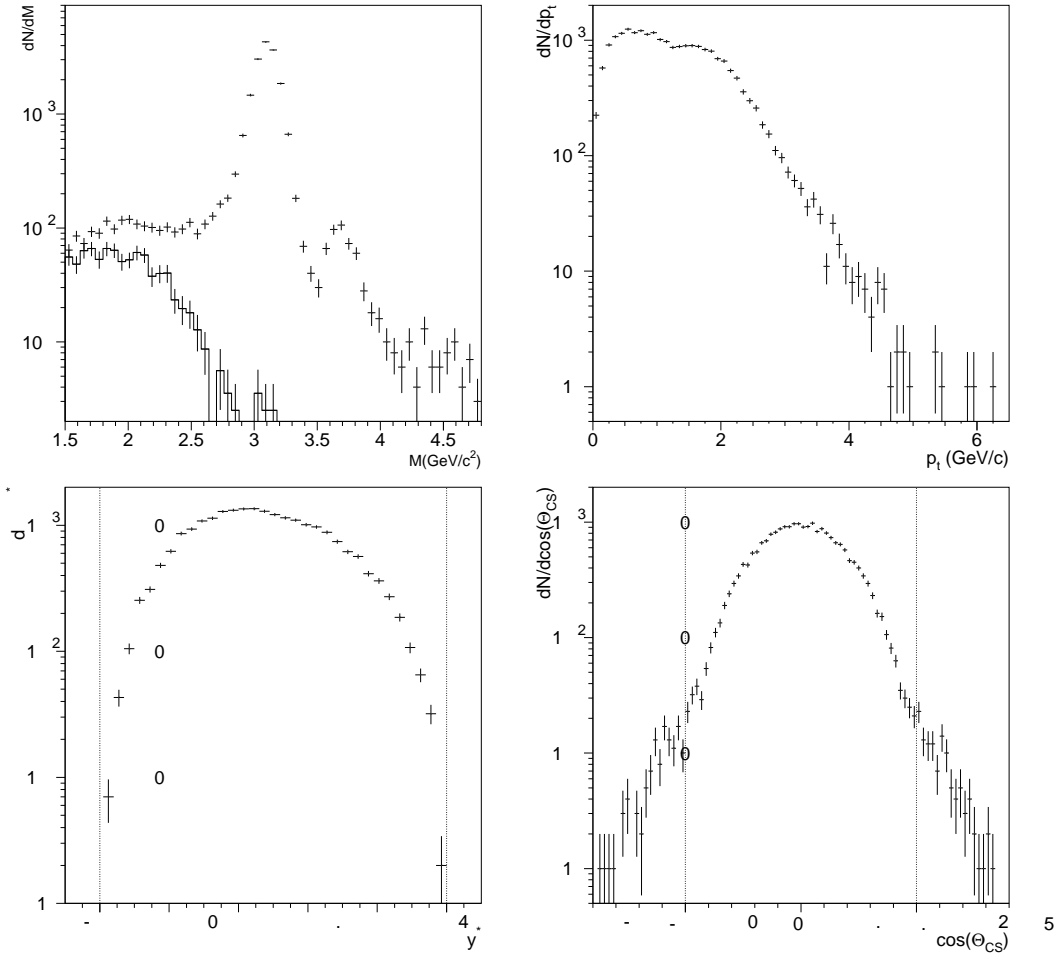


Figure 1: Dimuon mass, transverse momentum, rapidity and  $\cos(\theta_{cs})$  distributions, for the p-Cu (10.1) data set. The dimuon mass figure includes the background distribution.

angle relative to the beam line in the (Collins-Soper) dimuon reference frame. Figure 1 shows, as an example, the kinematical distributions of the muon pairs collected with the long Cu target. The final number of analysed  $J/\psi$  events varies between 2000 and 16 000. The exact values will be detailed in Table 4.

### 3 Analysis

The data analysis method followed in the present study is basically the same as used in the analysis of the S-U data, explained in Ref. [4]. The opposite-sign muon pair mass distributions are considered as a superposition of several contributions: the Drell-Yan dimuons, the decays from the  $J/\psi$  and  $\psi'$  vector mesons and the combinatorial

background due to  $\pi$  and K decays. Since we restrict the analysis to the mass region above  $2.9 \text{ GeV}/c^2$ , we have neglected the contribution from simultaneous semileptonic decays of charmed mesons.

The shapes of the DY,  $J/\psi$  and  $\psi'$  contributions to the dimuon mass spectra are determined by a simulation procedure that takes into account the acceptance and smearing effects due to the apparatus. The simulated events are reconstructed as the real data and have to survive the same selection cuts. Analytical functions optimized to provide a good parameterization of the simulated distributions [7] are used in the fit to the measured data, as shown in Fig. 2.

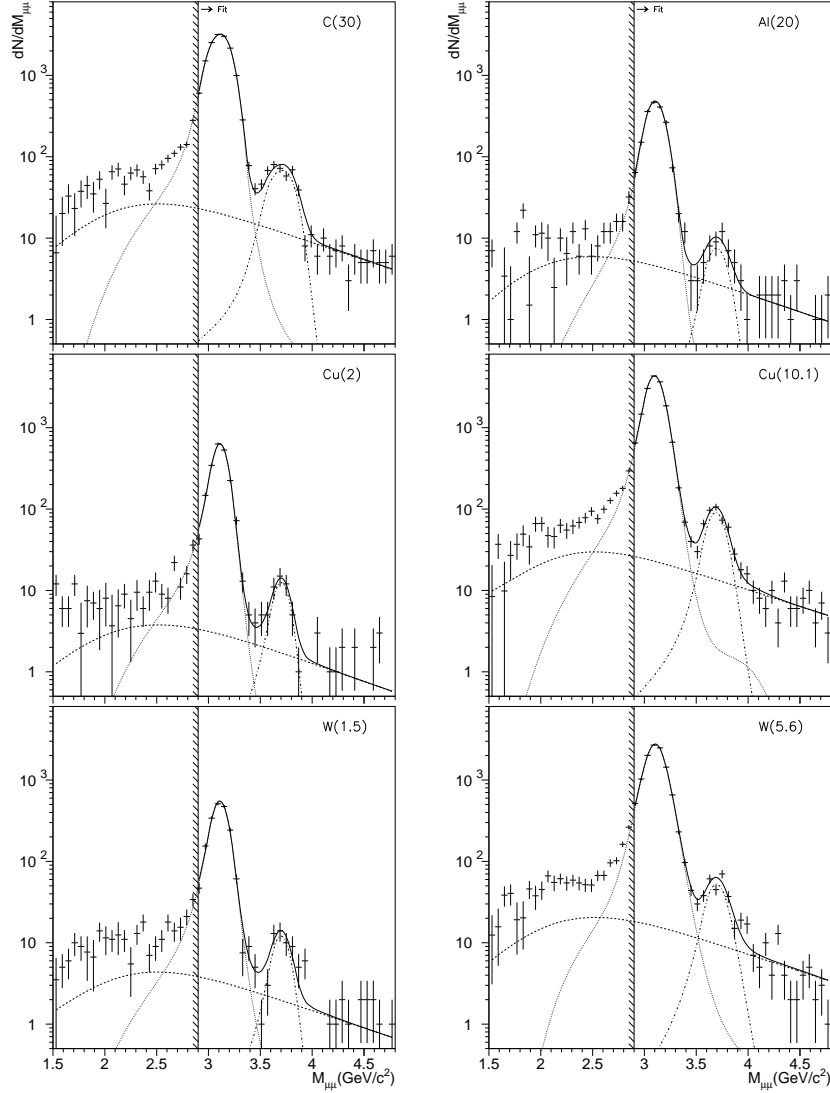


Figure 2: Mass spectra, after background subtraction, for the six data sets. The three components of the fit, performed in the mass window above  $2.9 \text{ GeV}/c^2$ , are also shown.

The simulation also provides the probability that the detector accepts the muon pairs resulting from  $J/\psi$  and  $\psi'$  decays, by making the ratio between the number of reconstructed and generated events, in our restricted kinematical window. The acceptances obtained are 12.1 % and 15.6 % for the  $J/\psi$  and  $\psi'$ , respectively. The change of target does not affect the dimuon acceptances in a significant way.

The fit procedure, performed in the mass window above 2.9 GeV/ $c^2$  after subtracting the background contribution, provides the number of Drell-Yan,  $J/\psi$  and  $\psi'$  events. In fact, the directly fitted quantities are the number of  $J/\psi$  events,  $N^\psi$ , and the particle ratios  $N^{\psi'}/N^\psi$  and  $N^\psi/N^{\text{DY}}$ . We will ignore the latter ratio in view of the rather small number of high mass events ( $M > 4$  GeV/ $c^2$ ) available in these data sets.

## 4 Ratio of charmonia cross sections

The ratio of charmonia cross sections in the dimuon channel,  $B_{\mu\mu}^{\psi'}\sigma^{\psi'}/B_{\mu\mu}^\psi\sigma^\psi$ , abbreviated in the following as  $\psi'/\psi$ , is free from systematic uncertainties related to the incident flux, target thickness, reconstruction inefficiencies, etc., since such factors affect in the same way both charmonium states and, therefore, cancel out in the ratio.

The ratio of accepted events,  $N^{\psi'}/N^\psi$ , is given directly from the fit to the mass distribution. After correcting this value by the ratio of acceptances, determined by the simulation procedure mentioned above, we obtain the ratios of cross sections presented in Table 2.

Table 2: Ratio of production cross sections, in the dimuon channel, for the measured p-A reactions. The average values from the two samples of Cu and W data are  $1.74\pm 0.11$  and  $1.59\pm 0.13$ , respectively.

	$N^{\psi'}/N^\psi$	$\psi'/\psi$ (%)
C	$2.45\pm 0.17$	$1.90\pm 0.13$
Al	$1.75\pm 0.45$	$1.36\pm 0.35$
Cu (2)	$2.15\pm 0.41$	$1.67\pm 0.32$
Cu (10.1)	$2.27\pm 0.16$	$1.75\pm 0.13$
W (1.5)	$2.38\pm 0.45$	$1.84\pm 0.35$
W (5.6)	$2.01\pm 0.18$	$1.55\pm 0.14$

The values obtained in this work are compared in Table 3 with other p-A results, obtained with different targets, beam energies and kinematical windows. The whole set of results is displayed on Fig. 3 as a function of A, the mass number of the target.

To quantify the dependence of charmonia production on the mass number of the target, the p-A cross sections are usually parameterized as  $\sigma_{\text{pA}} = \sigma_0 \times A^\alpha$ . From the  $\psi'/\psi$  values collected in Table 3, we can investigate if the production cross sections of the two charmonium states scale with A in the same way or not. Fitting the six

Table 3: Ratio of charmonia cross sections in the dimuon channel. The values obtained in this work are compared with previous results.

	$p_{\text{lab}}$ (GeV)	$\psi' / \psi$ (%)	Experiment
p-H	450	$1.57 \pm 0.04 \pm 0.02$	NA51 [8]
p-D	450	$1.67 \pm 0.04 \pm 0.025$	NA51 [8]
p-C	450	$1.90 \pm 0.13$	This work
p-Al	450	$1.36 \pm 0.35$	This work
p-Cu	450	$1.74 \pm 0.11$	This work
p-W	450	$1.59 \pm 0.13$	This work
p-W	200	$1.80 \pm 0.17$	NA38 [9]
p-U	200	$1.77 \pm 0.22$	NA38 [9]
pp	$\sqrt{s} = 63$	$1.9 \pm 0.6$	ISR [10]
p-Li	300	$1.88 \pm 0.26 \pm 0.05$	E705 [11]
p-Be	400	$1.7 \pm 0.5$	E288 [12]
p-Si	800	$1.65 \pm 0.20$	E771 [13]
p-Au	800	$1.8 \pm 0.1 \pm 0.2$	E789 [14]

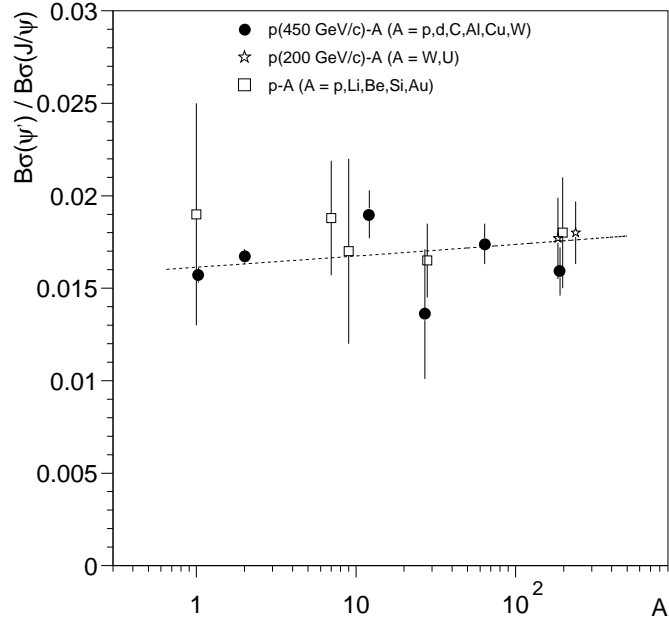


Figure 3: Ratio of charmonia cross sections in the dimuon channel as a function of the mass number of the target.



values measured at 450 GeV and in the same rapidity interval ( $-0.4 < y^* < 0.6$ ) with the function

$$\sigma_{\text{pA}}^{\psi'}/\sigma_{\text{pA}}^{\psi} = \sigma_0^{\psi'}/\sigma_0^{\psi} \times A^{\alpha^{\psi'} - \alpha^{\psi}}$$

leads to the values  $\sigma_0^{\psi'}/\sigma_0^{\psi} = 1.61 \pm 0.03$  % and  $\alpha^{\psi'} - \alpha^{\psi} = 0.014 \pm 0.011$ , with a  $\chi^2/\text{ndf}$  of 1.90. The result of the fit is drawn as a dashed line on Fig. 3.

This result is a strong indication that the  $J/\psi$  and  $\psi'$  cross sections scale in the same way with the target mass number, in p-A collisions. The agreement with measurements obtained under different conditions suggests that the  $\psi'/\psi$  ratio is independent of  $\sqrt{s}$  and rapidity, within the range explored by the experiments listed in Table 3.

## 5 Absolute cross sections

The  $J/\psi$  production cross section is derived from the number of detected  $J/\psi$  events, the incident flux, the acceptance of the detector for muon pairs from  $J/\psi$  decays and the efficiencies of the trigger hardware, of the acquisition system and of the offline reconstruction procedure. Table 4 presents, for each data set, the integrated luminosity already corrected for the appropriate efficiencies,  $\mathcal{L}$ , the number of detected events,  $N^{\psi}$ , and the corresponding cross section values.

Table 4:  $J/\psi$  and  $\psi'$  absolute cross sections, in the dimuon channel, for the measured p-A reactions. Systematic uncertainties, not included, amount to 7%.

	$\mathcal{L}$ (nb <sup>-1</sup> )	$N^{\psi}$	$B_{\mu\mu}^{\psi} \sigma^{\psi}$ (nb)	$B_{\mu\mu}^{\psi'} \sigma^{\psi'}$ (nb)
C	2232.5	15014 ± 140	55.8 ± 0.6	1.06 ± 0.07
Al	136.4	1851 ± 48	112.1 ± 2.8	1.52 ± 0.39
Cu (2)	63.0	2083 ± 51	267.8 ± 6.3	4.66 ± 0.31
Cu (10.1)	518.4	16522 ± 140	263.5 ± 2.4	4.58 ± 0.29
W (1.5)	25.4	1896 ± 48	606.1 ± 14.8	9.63 ± 0.77
W (5.6)	136.7	11533 ± 118	692.6 ± 7.4	11.00 ± 0.87

The absolute cross sections for  $\psi'$  production, also included in Table 4, were obtained from the  $J/\psi$  values and from the  $\psi'/\psi$  ratios given in Table 3.

Besides the statistical errors included in Table 4, the absolute cross sections are affected by a 7% systematical uncertainty due to the luminosity measurement. This error bar arises from uncertainties in the trigger efficiency and in the absolute calibration of the ionisation chamber that measures the intensity of the beam, affecting in the same way all the data sets. Therefore, it should not be included in relative comparisons of the values obtained from the different targets.

From the cross section values reported in Table 4 and the target mass numbers collected in Table 1, we can derive the  $J/\psi$  cross section per nucleon,  $B_{\mu\mu}^{\psi} \sigma^{\psi}/A$ . The

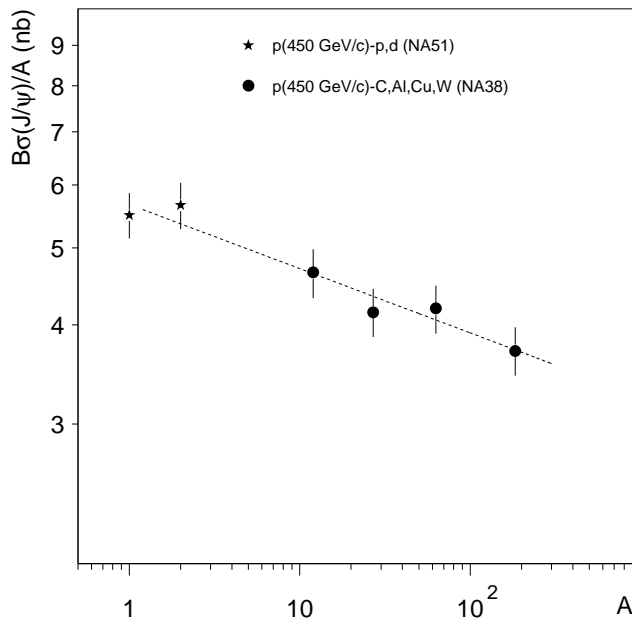


Figure 4: Absolute  $J/\psi$  cross sections per nucleon as a function of the mass number of the target. The dashed line corresponds to the  $A^\alpha$  parametrization fitted to the data.

resulting values are  $4.65 \pm 0.04$ ,  $4.15 \pm 0.10$ ,  $4.19 \pm 0.04$  and  $3.71 \pm 0.04$  nb, for the C, Al, Cu and W targets, respectively. They are displayed in Fig. 4, together with the NA51 values [8],  $5.50 \pm 0.36$  nb for p-H and  $5.66 \pm 0.38$  nb for p-D.

The departure of the points from a flat line reveals that  $\alpha^\psi$  is lower than unity, contrary to what has been observed for the Drell-Yan mechanism. Indeed, fitting the two sets of points with the  $A^\alpha$  parameterization, we obtain

$$\alpha^\psi = 0.919 \pm 0.015$$

with a  $\chi^2/\text{ndf}$  of 0.38. Since the systematic effects are not the same in the two experiments, the systematic uncertainties have been included in the fit.

## 6 Conclusion

We have measured the  $J/\psi$  and  $\psi'$  production cross sections with a 450 GeV proton beam incident on C, Al, Cu and W targets. The results obtained in this experiment, together with those obtained with the same beam energy and a similar detector for p-H and p-D reactions, provide a strong indication that the ratio of cross sections for these two charmonia states is independent of the mass number of the target, in our kinematical window. The usual power-law parametrisation of the A-dependence

provides a good description of the data with  $\alpha^\psi = 0.919 \pm 0.015$  and  $\alpha^{\psi'} - \alpha^\psi = 0.014 \pm 0.011$ . The comparison with results obtained by other experiments strongly suggests that the  $\psi'/\psi$  ratio has no significant dependence on the proton incident momentum, at least in the range between 200 and 800 GeV [15].

The results reported in this paper provide a significant constrain on models that attempt to explain the charmonia suppression observed in nucleus-nucleus collisions [4, 5] by interactions of fully formed  $J/\psi$  and  $\psi'$  states with comoving hadrons. In particular, our results are in clear disagreement with the monotonic decrease predicted in Refs. [16, 17] for the  $\psi'/\psi$  ratio, of more than 20 % between p-D and p-W.

## References

- [1] D.M. Alde *et al.*, Phys. Rev. Lett. **66** (1991) 133.  
R. Cases Ruiz, Ph.D. Thesis, Universitat de Valencia (1989).  
J. Badier *et al.*, Z. Phys. **C 20** (1983) 101.  
K.J. Anderson *et al.*, Phys. Rev. Lett. **42** (1979) 944.  
J.G. Branson *et al.*, Phys. Rev. Lett. **38** (1977) 1334.  
M. Binkley *et al.*, Phys. Rev. Lett. **37** (1976) 571.
- [2] T. Matsui and H. Satz, Phys. Lett. **B 178** (1986) 416.
- [3] L. Fredj, Ph.D. Thesis, Clermont-Ferrand (1991).
- [4] M.C. Abreu *et al.* (NA38 Coll.), in preparation.
- [5] M.C. Abreu *et al.* Phys. Lett. **B 410** (1997) 327.
- [6] L. Anderson *et al.*, Nucl. Instrum. Meth. **223** (1984) 26.
- [7] F. Fleuret, Ph.D. Thesis, Ecole Polytechnique (1997).
- [8] M.C. Abreu *et al.* (NA51 Coll.), accepted by Phys. Lett. B.
- [9] C. Lourenço, Ph.D. Thesis, Universidade Técnica de Lisboa (1995).
- [10] A.G. Clark *et al.*, Nucl. Phys. **B 142** (1978) 29.
- [11] L. Antoniazzi *et al.*, Phys. Rev. **D 46** (1992) 4828.
- [12] H.D. Snyder *et al.*, Phys. Rev. Lett. **36** (1976) 1415.
- [13] T. Alexopoulos *et al.*, Phys. Lett. **B 374** (1996) 271.
- [14] M.H. Schub *et al.*, Phys. Rev. **D 52** (1995) 1307.
- [15] C. Lourenço, Nucl. Phys. **A610** (1996) 552c.
- [16] A. Capella *et al.*, Phys. Lett. **B 393** (1997) 431.
- [17] D.E. Kahana and S.H. Kahana, preprint nucl-th/9808025 (1998).